Ore Geology Reviews 73 (2016) 417–431

Contents lists available at ScienceDirect

Ore Geology Reviews

journal homepage: www.elsevier.com/locate/oregeorev

Geochemical challenges of diverse regolith-covered terrains for mineral exploration in China

Wang Xueqiu [b,c,*], Zhang Bimin [a,c], Lin Xin [a,c], Xu Shanfa [a,c], Yao Wensheng [a,c], Ye Rong [b,c,*]

[a] Institute of Geophysical and Geochemical Exploration, CAGS, Langfang 065000, China
[b] China University of Geosciences (Beijing), Beijing 10083, China
[c] Key Laboratory of Geochemical Exploration, Ministry of Land and Resources, Langfang 065000, China

ARTICLE INFO

Article history:
Received 15 September 2014
Received in revised form 8 July 2015
Accepted 19 August 2015
Available online 28 August 2015

Keywords:
Regolith
Nano-crystal particles
Gold
Copper
Uranium

ABSTRACT

In recent years mineral exploration has concentrated on concealed deposits in regolith-covered terrains. In China, the regolith-covered landscapes mainly include desert windblown sand basins, desert peneplains, semi-arid grassland, loess plateaus, forestry land, alluvial plains and laterite terrains. These diverse regolith-covered areas represent geochemical challenges for mineral exploration in China. This paper provides an overview of recent progress on mechanisms of metal dispersion from the buried ore deposits through the transported cover to the surface and penetrating geochemical methods to detect the anomalies. Case studies show that, in arid and semi-arid desert sand-covered terrains, sampling of fine-fraction (−120 mesh, <0.125 mm) clay-rich horizon soil is cost-effective for regional geochemical surveys for sandstone-type uranium, gold, and base metal deposits. Fine-fraction sampling, selective-leaching and overburden drilling geochemical methods can effectively indicate the 210 gold ore body at Jinwozi goldfield. In alluvium-covered terrains, fine-grained soil sampling (−200 mesh, <0.074 mm) combined with selective leaching geochemistry shows clear ring-shaped anomalies of Cu and Ni over the Zhouan concealed Cu–Ni deposit. In laterite-covered terrains, the anomalies determined by the fine-fraction soils and selective leaching of absorbed metals on coatings of Fe–Mn oxides coincide well with the concealed deposit over the Yueyang ore deposits at the Zijin Au–Cu–Ag field. Nanoparticles of hexagonal crystals mainly native copper, gold and alloys of Cu–Fe, Cu–Fe–Mn, Cu–Ti, and Cu–Au were observed in gases, soils and ores using a transmission electron microscope (TEM). The findings imply that nanoparticles of gold and copper may migrate through the transported cover to the surface. Uranium is converted to uranyl ions [UO_2^{2+}] under oxidizing conditions when migrating from ore bodies to the surface. The uranyl ions are absorbed on clay minerals, because clay layers have a net negative charge, which needs to be balanced by interlayer cations. Nanoparticles of Au and Cu and ion complexes of U are more readily absorbed onto fine fractions of soils containing clays, colloids, oxides and organic matters. Thus, fine-grained soils enriched with clays, oxides and colloids are useful media for regional geochemical surveys in regolith-covered terrains and in sedimentary basins. Fine-fraction soil sampling combined with selective leaching geochemistry is effective for finding concealed ore bodies in detailed surveys. Penetrating geochemistry at surface sampling provides cost-effective mineral exploration methods for delineation of regional and local targets in transported cover terrains.

1. Introduction

Geochemical exploration has played an important role in mineral discoveries, particularly due to China's National Geochemical Mapping Program — Regional Geochemistry-National Reconnaissance (RGNR). The program is almost covering all the outcropping mountainous and hilly areas (approximately 6 million km^2) mainly using stream sediment sampling (Xie et al., 1997). However, the diverse regolith-covered terrains provide an additional geochemical challenge for mineral exploration in China. In recent years, nation-wide mineral exploration activities are now concentrating on concealed deposits in regolith-covered terrains. Particularly in the new century, interest was kindled by the discoveries of the large porphyry copper deposits and large sandstone-type uranium deposits in Gobi desert terrains extending from northern China northward into Mongolia. For example the large copper porphyry deposit located at Tuwu in the Eastern Tianshan Gobi (Fig. 1) (Wang et al., 2007a), the large copper and gold porphyry deposits located at Oyuu Tolgoi, about 80 km from the Chinese border into Mongolia (www.ivanhoe-mines.com) and large sandstone-type uranium deposits at the Turpan–Hami Basin (Quan and Li, 2002) and at Ordos Basin (Dahlkamp, 2009).

* Corresponding authors at: China University of Geosciences (Beijing), Beijing 10083, China.
E-mail addresses: wangxueqiu@igge.cn (W. Xueqiu), yerong@cugb.edu.cn (Y. Rong).

http://dx.doi.org/10.1016/j.oregeorev.2015.08.015
0169-1368/

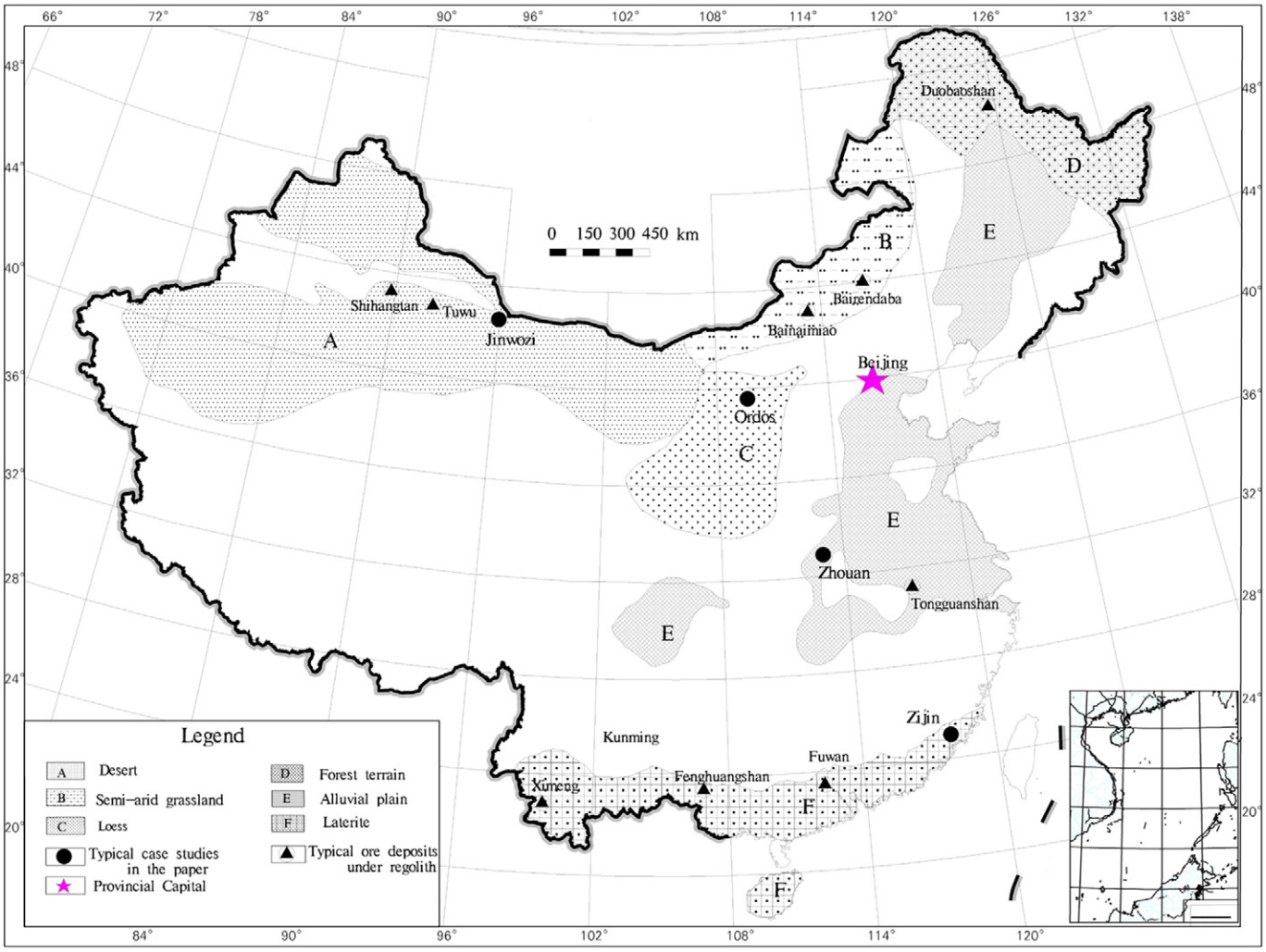

Fig. 1. Regolith-covered terrains with locations of case studies and some typical large ore deposits in Chinese covered terrains.

Table 1
Main features of different types of regolith-covered terrains.

Types of regolith	Estimated total surface (km^2)	Cover thickness range (m)	Climate & vegetation
Gobi desert (A)	1,435,000	A few meters to tens of meters at desert peneplains, more than 10 m at desert basins	i) Arid; ii) Average rainfall less than 200 mm; iii) Barren, sparse vegetation, shrub & alhagi-rich
Semi-arid grassland (B)	323,900	A few meters to tens of meters, an average of less than 10 m	i) Semi-arid continental climate; ii) Average rainfall of 300 mm; iii) Dominated by grass; iv) Chestnut soil well-developed;
Loess (C)	385,000	A few meters to more than 600 m, an average of 50–80 m	i) Semi-arid to semi-humid; ii) Average rainfall of 500 mm; iii) Broad-leaved and coniferous forests of temperate zone, farmland;
Forest terrain (D)	391,000	A few meters to tens of meters, an average of less than 10 m	i) Humid; ii) Average rainfall of 500–1000 mm; iii) Arbor-rich, humus well-developed; iv) Large areas of perpetually frozen soil; v) Broad-leaved and coniferous forests of frigid zone vi) Marsh areas widely distributed;
Alluvial plain (E)	996,200	A few meters to hundreds of meters, with a maximum of more than thousands of meters	i) Monsoon climate of medium latitudes; ii) Average rainfall of 500–1000 mm; iii) Farmland;
Laterite (F)	463,000	A few meters to tens of meters, an average of less than 10 m	i) Subtropical to tropical rain forest; ii) With average rainfall of 1800 mm; iii) Broad-leaved forest; iv) Soils enriched in iron and aluminum oxides.

A, B, C, D, E and F have the same meanings with those in Fig. 1.

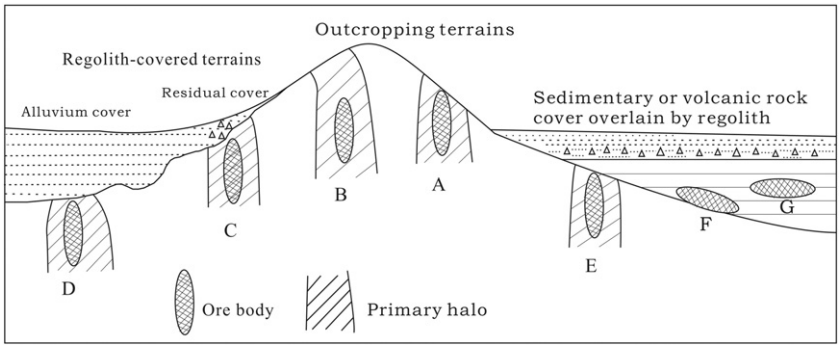

Fig. 2. Sketch showing seven occurrence types of ore deposits. A—exposed, B—concealed in bed rocks, C—covered by residuum, D—buried by transported soils, E—covered by post-mineralization covers, F—concealed by volcanic or sedimentary rock and overlying regolith, G—hosted by sedimentary rocks and overlying regolith.

Traditional geochemical methods, for example, litho- and stream-sediment geochemistry, are inadequate because mineral deposits are covered by various cover materials (e.g. Quaternary regolith) where rock or stream sediment samples are not available. A variety of new approaches corresponding to numerous successful case studies have been introduced, such as the geogas method (Cao, 2001; Kristiansson and Malmqvist, 1982; Kristiansson et al., 1990; Malmqvist and Kristiansson, 1985; Malmqvist et al., 1999; Ren et al., 1995; Tong et al., 1991; Tong and Li, 1999; Wang et al., 1995a, 1997, 2006a, 2006b; Wang, 1999; Xie et al., 1999; Ye et al., 2004), enzyme leach (Bajc, 1998; Clark and Meier, 1990; Clark, 1993; Clark et al., 1997; Hall, 1998; Williams and Gunn, 2002; Yeager et al., 1998), mobile metal ion (Gray et al., 1999; Mann et al., 1995), sequential leaching of mobile forms of metals in overburden (Wang, 1998a; Xie and Wang, 2003), electrogeochemical (Antropova et al., 1992; Ryss and Goldberg, 1973; Smith et al., 1993; Luo et al., 1999, 2008) and biogeochemical methods (Anand et al., 2007; Erdman and Olson, 1985; Ozdemir, 2005), therefore, the term deep-penetrating geochemistry was coined at the right time (Wang, 1998a, 1998b; Xie and Wang, 2003; Cameron et al., 2002, 2004).

We have little understanding of vertical migration mechanisms of different elements from buried ore bodies upwards through diverse transported covers to the surface. In this paper, the authors will give an overview of recent typical case histories in different covered terrains of China on metal migration mechanism that penetrates the exotic cover and on the most successful exploration protocols for representative case studies.

2. Regolith-covered terrains and concealed mineral deposits in China

2.1. Diverse regolith-covered terrains in China

China lies between latitudes 18° and 54° N, and longitudes 73° and 135° E. Consequently China's regolith-covered terrains vary significantly as shown in Fig. 1. The regolith-covered terrains mainly include arid deserts (Gobi desert), loess plateaus, forest and swamps, alluvial plains, semi-arid grasslands and laterite. Northern and north-western China is dominated by windblown sand-covered terrains including the arid desert basins, desert peneplains, semi-arid grassland and loess plateaus, where the soils are composed mostly of windblown sand. This could dilute the contents of mineralized elements and mask the signals of mineralization. Most area of Northeast China is well developed with forest and swamp and covered by thick soils with high concentrations of organic materials. East China is covered by alluvial soils that conceal bedrocks and any ore deposits. South China is predominated by laterite terrain where red earth and laterite are enriched in many elements by the process of chemical decomposition of these rocks and residual concentrations. These diverse regolith-covered terrains are under-explored or even unexplored; in addition, they are the current geochemical challenges for mineral exploration in China (Table 1).

2.2. Categories of mineral deposits

Fig. 2 illustrates the major categories of mineral deposits in light of exploration geochemistry. Type A is exposed deposit and type B is concealed by outcropping bedrocks. The other five are concealed by post-mineralization cover such as sedimentary rocks, volcanic rocks and regolith.

Deposits of type A, with outcropping mineralization and wall rocks are the easiest to be discovered by prospectors even with naked eye due to natural exposure at the Earth's surface. Ore bodies could be intersected by drainage systems and the components of ore bodies can be mechanically transported into stream sediments. Therefore, basic litho-geochemical and stream sediment geochemical surveys are effective for identifying these anomalies.

Type B deposits are concealed in host rocks. The signals of mineralization can be recognized by their alteration signatures, or by rock geochemical surveys for leakage halos and by analysis of pathfinder trace elements.

Type C deposits are covered by a veneer of residuum. Although the probability of finding this deposit by direct observation is greatly reduced, the release of metals during chemical weathering can lead to dispersion of mineralization elements in the residuum. Soil geochemical surveys here are effective to find this kind of ore deposit. The weathering products of type A, B and C are easily transported into drainage systems and will give rise to a detectable anomaly. Thus there is also an excellent chance of discovering these deposits with regional reconnaissance stream sediment geochemical surveys

Table 2
Summary of the four deposits in the case studies.

Mineral deposit	Tonnage (ton)	Type	Date (year), depth (m), method of discovery	References
210 Au deposit	10	Ductile-shear type Au deposit	1993, 10–20 m, regional geochemical survey	Chen et al. (1999)
Zhou'an Cu–Ni deposit	445,900	Post-magmatic hydrothermal Cu–Ni deposit	2006, 400–700 m, airborne magnetic anomalies	Wang et al. (2006a, 2006b); Yan et al. (2011)
Yueyang–Bitian Ag–Au–U deposit	1000	Epithermal Ag–Au deposit	1990, 170–460 m, regional geochemical survey	Chen et al. (1997, 1998); Wang et al. (2009)
Ordos uranium deposit	20,000	Sandstone-type U deposit	2000, <100 m, radiometric survey	Liu et al. (2006); Dahlkamp (2009)

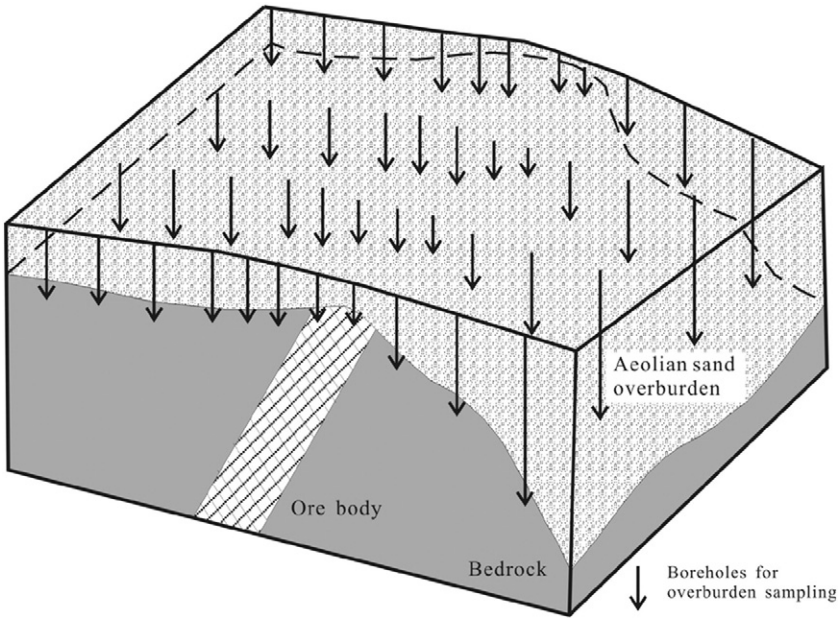

Fig. 3. Simplified geological model of the Jinwozi gold ore body covered by windblown sand indicated by drilling.

The type D deposits are completely covered by exotic transported soils. Here, geochemical exploration techniques on either a regional or detailed basis, as presently practiced, offer little promise of discovery, although there has been some success with the sampling of groundwater, vegetation, basal caliche layers and vapors.

The type E deposit is concealed by various post-mineralization covers which include volcanic and sedimentary rocks, alluvium and weathered cover. The thick sequence of overlying covers will completely mask both underlying prospective bedrock sequences and expressions of concealed deposits. Here, geochemical exploration techniques presently available are unlikely to succeed.

The type F deposits are hosted at the bottom of volcanic rocks, above which transported cover is also well-developed.

The type G deposits are hosted by sedimentary rocks. Most sandstone-type uranium deposits at the basins belong to this type.

Types of D, E and F, G are unlikely to be detected by conventional geochemical methods as now generally practiced. However, the resource potential of concealed deposits could be greater than that of the exposed deposits, so the development of methods for their discovery is the real geochemical challenge for the present and future.

3. Case studies

This section gives 4 typical case studies from the above-mentioned regolith-covered terrains in China (Table 2). The reasons for choosing these four case studies are that they could provide the reader with a perspective of both regional- and local-scale geochemical exploration for different types of concealed deposits. Sampling, preparation and laboratory analysis carried out for this study can be found in Wang (1998b, 1999), Wang et al. (1997, 2007a, 2007b, 2011, 2014) and Zhang et al. (2013).

3.1. The Jinwozi goldfield — covered by windblown sand

The 210 gold deposit lies in the Jinwozi goldfield in the Gobi desert in Xinjiang, north-western China (Fig. 1). The gold veins mainly occur within a ductile shear zone that trends northeast and dips northwest at 10–40°. Metamorphosed tuff, volcanoclastic rocks and sandstone are the major host rocks of the 210 deposit. The main wall rock alterations are sericitization, pyritization, silicification and chloritization. Native gold, electrum, pyrite and arsenopyrite are the major ore minerals, and chalcopyrite, sphalerite and galena are the minor ones (Lin et al., 2014a). The deposit is covered by four to several tens of meters of Tertiary to Quaternary regolith and sediments as indicated by drilling (Fig. 3). The sequence of the regolith materials from bottom to top can be summarized as follows: weathered bedrock, coarse sand, sand and gravel, sandy clay and desert crust of gravel (Wang et al., 2007a).

Studies having been conducted since 1999 were aimed at understanding the geochemical dispersion in order to find a wide-spaced sampling method to delineate geochemical provinces and a detailed geochemical sampling method for locating the ore bodies. The field experimental results show that gold tends to be concentrated in the fine-grained soil fraction (−120 mesh, <0.125 mm) at a depth of 150–300 mm. Powder diffraction analysis was applied to acquisition of mineral compositions (Table 3).

Table 3
Results of X-ray powder diffraction analysis of different soil fractions in the Jinwozi area.

Grain size (mesh)	Minerals (%)								
	Quartz	Orthoclase	Plagioclase	Calcite	Kaolinite	Illite	Chlorite	Amphibole	Gypsum
+20	32.4	15.4	17.6	8.3	0.4	5.4	1.9	0.9	14.6
−20–+40	19.7	11.3	12.9	15.5	0.6	7.6	3.3	–	24.3
−40–+60	18.7	6.3	18.1	9.4	0.6	7.1	3.5	–	30.6
−60–+80	23.9	4.0	9.5	11.4	0.9	10.6	3.7	–	31.0
−80–+100	15.4	3.2	10.1	15.3	1.3	13.8	5.2	1.5	24.7
−100–+120	13.9	5.5	8.6	21.9	2.2	18.8	8.6	0.7	16.4
−120	13.6	3.5	5.9	19.8	2.9	26.8	11.2	0.8	9.0

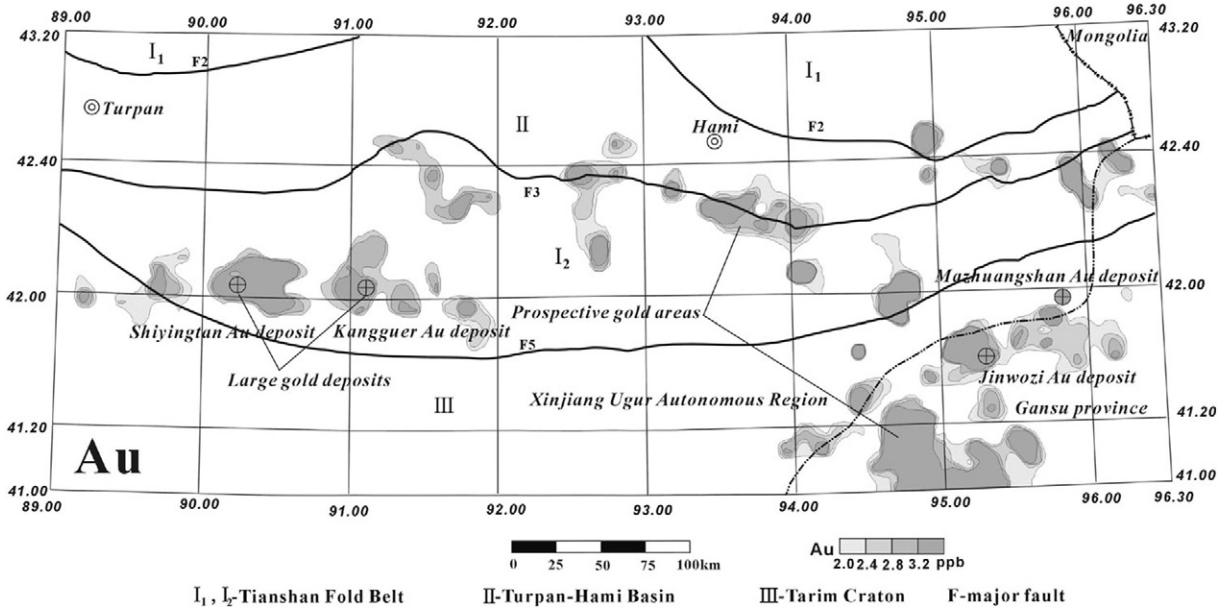

Fig. 4. Geochemical provinces delineated by fine-fraction (−120 mesh) sampling at a density of 1 sample/100 km^2 (Wang et al., 2007b).

Therefore, in eastern Tianshan region, fine-grained fraction (−120 mesh) of regolith samples at a depth of 150–300 mm enriched in clay minerals (Table 3) was collected at a density of 1 sample per 100 km^2. The samples were analyzed by XRF and ICP-MS after a hot 4-acid treatment. Geochemical provinces in the Jinwozi goldfield and Shiyingtan region were delineated (Fig. 4) (Wang et al., 2007b). Table 4 summarizes the statistical parameters.

Table 4
Statistical parameters of regolith samples collected in eastern Tianshan.

Elements	Minimum	Maximum	Average	St. dev.	Background
Ag	13.0	1171.0	60.7	67.5	37.0
As	1.5	197.8	9.8	7.5	6.7
Au	0.1	306.5	3.0	9.8	2.0
Cu	3.8	101.2	20.3	8.6	13.2
Hg	2.8	706.6	10.2	24.1	4.4
Mo	0.3	40.0	1.3	1.3	0.7
U	0.9	12.8	3.2	1.0	2.1

Note: Ag, Au, Hg in ng/g, others in μg/g.

Furthermore, samples of fine-grained soil fractions (−160 mesh, <0.088 mm) at a depth of 150–300 mm were taken at a density of 1 sample/6 km^2 at the Jinwozi goldfield. The samples were subjected to the analysis of XRF and ICP-MS after a 4-acid treatment. The results show a significant NE-trending gold anomaly coincident with the ductile-shear zone hosting the 210 gold deposit (Fig. 5).

Samples of different soil fractions at different depths (A > 0.833 mm (+20 mesh), 0.088 mm (160 mesh) < B < 0.833 mm (+20 mesh), C <0.088 mm (−160 mesh) mm in Fig. 6) were taken along a transect over the 210 deposit using improved Rotary Air Blast (iRAB) drilling. XRF and ICP-MS after a 4-acid treatment were used to obtain geochemical contents. A gold geochemical pattern indicated that the fine-grained fraction (grain-size < 0.088 mm (−160 mesh), C in Fig. 6) delivers stronger (with most Au anomalous value > 10 ppb) and relatively consecutive anomalies over the deposit compared to those of relatively coarse grained fractions (with most Au anomalous value between 3 and 10 ppb) (A and B in Fig. 6), and that gold is concentrated at the bottom and at the surface with low concentrations in the middle (Lin et al., 2014b). In addition, samples of grain-size smaller than 0.088 mm

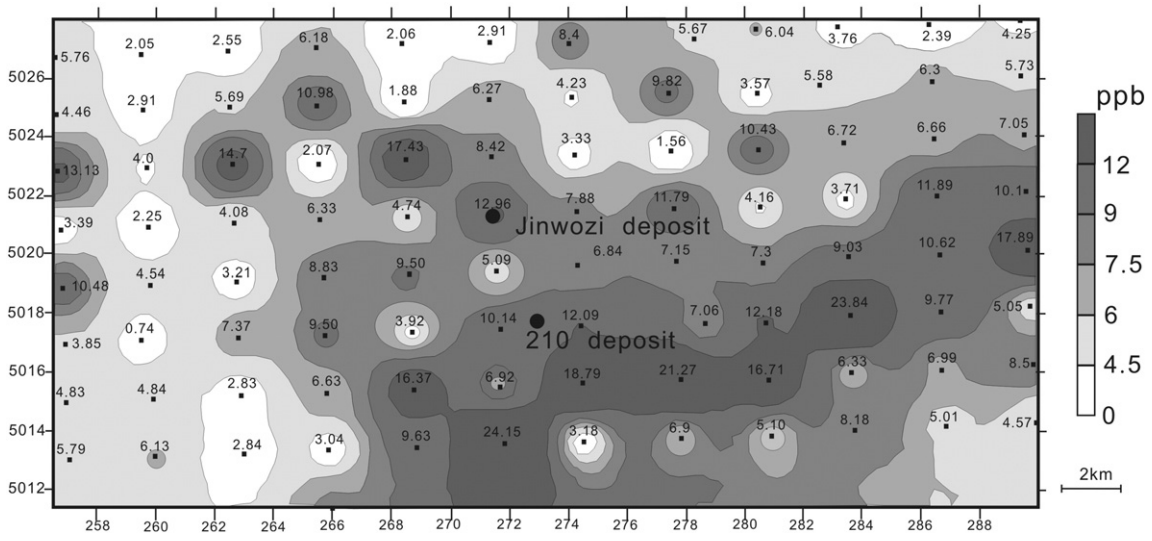

Fig. 5. Regional geochemical anomalies delineated by fine-fraction sampling at a density of 1 sample/6 km^2.

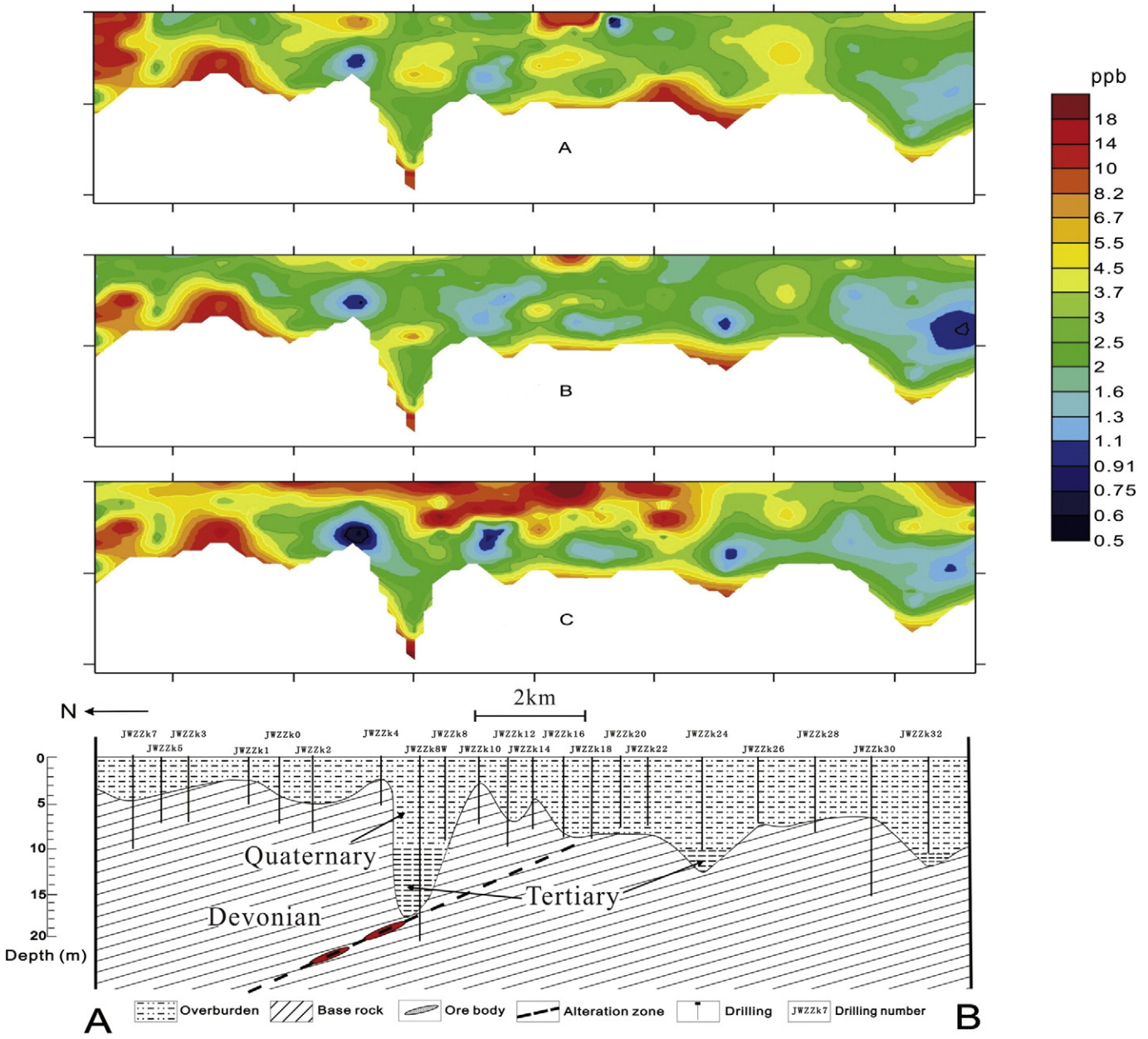

Fig. 6. Geochemical patterns of gold delineated by different fractions of soil samples at different depths over the 210 deposit (notation: X axis—sample number, Y axis—gold concentration (ppb), A: >0.833 mm (+20 mesh), B: 0.088 mm (160 mesh) < B < 0.833 mm (20 mesh), C: <0.088 mm (−160 mesh)).

(160 mesh) have the highest background value of Au at 8.2 ng/g and the biggest contrast of background and anomaly. Contrarily, samples of grain-size between 160 mesh and 20 mesh have both the smallest background value of Au at 3.8 ng/g and the contrast of background and anomaly.

The above results show that sampling of fine fraction of soil is more effective in delineation of regional and local gold geochemical anomalies for windblown sand regolith-covered deposits. Robertson (1999) has obtained similar results in the northeast Yilgarn Craton of Western Australia. The fine-grained size may vary from area to area for the case studies in this paper. The fine-grained fraction is generally defined as soil grain minus 100 mesh (0.150 mm) enriched clay minerals in this paper.

3.2. Zhou'an Cu–Ni deposit — covered by sedimentary rocks and alluvial soils

The Zhou'an Cu–Ni deposit is located 29 km south of Tanghe County, Henan province. The ore-bearing ultramafic complex with extensive alteration has been intruded into Mesoproterozoic and Neoproterozoic metamorphic strata. The stratiform ore bodies, mainly at the top and bottom of the complex, were formed by post-magmatic hydrothermal processes (Mi et al., 2009). The complex and its ore bodies are buried under Cenozoic strata and Quaternary alluvial soils at a depth of more than 400 m (Fig. 7). Traditional geochemical surveys are useless under these circumstances. However, airborne magnetic anomalies contributed largely to the discovery of the Zhou'an Cu–Ni deposit. It is an ideal area for a deep-penetrating geochemistry study as there have been no signs of any exploitation and contamination (Zhang et al., 2013).

Sampling of fine-grained fraction of soil (−200 mesh, <0.074 mm) at a depth of 100–300 mm coupled with selective leaching (Wang, 1998a, 1998b) was utilized on 5 traverse lines over the Zhou'an concealed Cu–Ni deposit. A clear ring-shaped anomaly of Cu was identified right over the deposit (Fig. 8). In addition, Tables 5 and 6 summarize the analytical results of X-ray diffraction and statistical parameters of fine-grained soil samples at the Zhou'an deposit respectively.

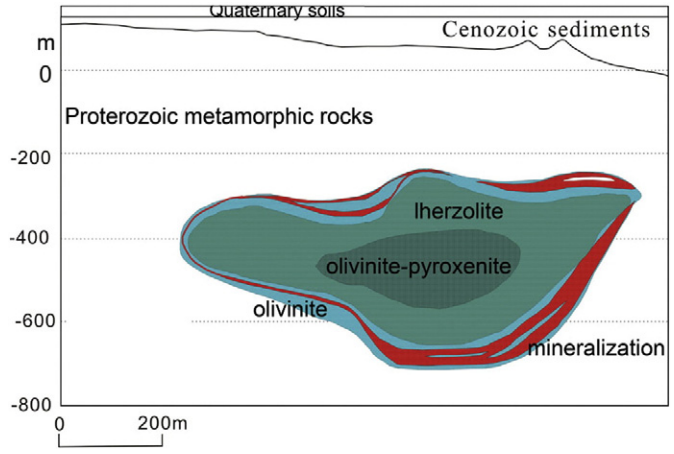

Fig. 7. Simplified geological model of the Zhou'an Cu–Ni deposit and its hosting ultramafic complex under Cenozoic strata and Quaternary alluvial soils at a depth of more than 400 m.

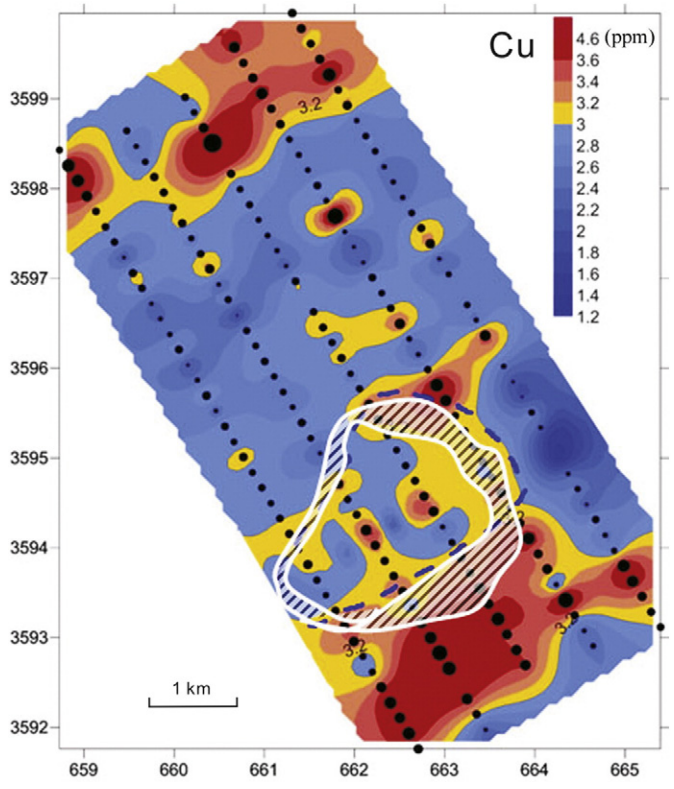

Fig. 8. Ring-shaped anomaly of Cu over the Zhou'an Cu–Ni deposit (Wang et al., 2012).

3.3. Yueyang Bitian Ag–Au–U deposit at Zijin in a laterite terrain

The Zijin copper–gold ore field is one of the main Cu–Au producers in Fujian province, southeastern China (Fig. 1) (Yu et al., 1995). Different types of deposits, including the Yueyang Bitian epithermal Ag–Au–U ore deposit, the Zijinshan middle-low temperature hydrothermal Cu–Au deposit and the Luoboling porphyry Cu–Mo deposit are distributed from the southwest to the northeast (Fig. 9). The Bitian Ag–Au–U deposit is completely covered by volcanic rocks overlain by laterite. Fine-grained soil fraction (−200 mesh, <0.074 mm) samples at a depth of 50–200 mm were taken on a traverse across the deposit (Zhang et al., 2013). XRF and ICP-MS after a 4-acid treatment for total digestion and selective sequential leach were used. Fig. 10 shows that the anomalous distribution of the fine fraction soils after 4-acid and aqua regia extraction and ammonium citrate plus hydroxylamine hydrochloride extraction of the coatings of Fe–Mn oxides (FMM) coincide well with the concealed deposit and the contrast of background and anomaly is strong. From the southwest to the northeast, anomalies of analyzed elements show horizontal zoning: (As–Sb–Hg–Ag–Au–U) → (Ag–Au–Pb–Zn–Bi–Cu) → (Mo–Cu–Zn–U–W), which spatially correlates to the corresponding mineral deposits.

3.4. Sandstone uranium deposits in basins

Regional geochemical stream sediment surveys have been used to investigate hilly and mountainous areas. Basins and adjacent areas have long been neglected. Researchers in China commenced regional geochemical survey in basins in 1999 under the project 'Low density deep-penetrating geochemical survey in arid desert of eastern Tianshan region' using fine fraction clay-rich soil samples (−120 mesh, <0.125 mm) at a depth of 200–400 mm combined with sequential selective leach (Wang et al., 2011). Summaries of parameters of geochemical data can be found in Table 4. This has obtained satisfactory results at Terpan–Hami Basin, northwestern China (Fig. 11) (Wang et al., 2007b, 2011). A known U deposit, Shihongtan, occurred among the resultant anomalies and two prospective areas for sandstone U deposits were targeted.

Fine fraction sampling was also applied to a regional uranium survey in the Ordos Basin with an area of 23,104 km^2 (Yao et al., 2012). The Ordos sandstone-type U deposit occurs in Jurassic sandstone, and is covered by Cretaceous strata and soil. The designed sampling density was 1 site/4 km^2. The fine fraction (−100 mesh, <0.147 mm) of the catchment soil samples at a depth of around 150 mm was collected in the field and later sieved to −200 mesh (<0.074 mm) in the laboratory for total analysis and selective leach by XRF and ICP-MS (Yao et al., 2012). Table 7 summarizes the statistics of geochemical data from fine fraction soil samples at Ordos Basin, Inner Mongolia, northern China. The resultant anomalies can be closely correlated to the belt of sandstone uranium mineralization (dashed line in Fig. 12).

Table 5
Results of X-ray diffraction of fine-grained soil samples at the Zhou'an deposit.

Sample no.	Minerals (%)						
	Quartz	Montmorillonite	Orthoclase	Plagioclase	Illite	Kaolinite	Calcite
1	43–47	30	5	5–10	5	1–2	1
2	44–49	30	3	5–10	3	1–2	1
3	55–59	25–30	3	5	1–2	1–2	1
4	55	25–30	3	5–10	–	1–2	1
5	53–50	30	3–5	5–10	–	2–3	–
6	48–52	25–30	3	10	3	2–3	–
7	44–45	30	3	10	1–2	2–3	3–5
8	52–53	25–30	3	5–10	1–2	2–3	1–2

Table 6
Statistical parameters of fine-grained soil samples at the Zhou'an deposit.

Elements	Minimum	Maximum	Average	St. dev.	Background
Co	7.5	74.9	14.4	5.26	13.7
Cr	54.9	354.4	79.9	20.79	77.5
Cu	15.7	92.3	24.8	7.29	23.5
Ni	17.3	82.2	30.8	7.75	29.7
Pb	16.8	190.6	28.9	12.82	27.3
Zn	35.4	279.5	60.3	23.80	57.0
TFe_2O_3	3.09	11.87	4.80	1.18	4.59

Note: TFe_2O_3 in %, others in μg/g.

4. Migration mechanism of elements through transported cover

4.1. Overview of migration mechanism

Dispersion of metals from concealed mineralization can superimpose anomalies on the transported cover at or near surface. It is generally thought that trace elements are transported to the surface by one or more of the following mechanisms: (i) groundwater flow (Cameron, 1998; Cameron et al., 2002, 2004; van Geffen et al., 2012; Leybourne and Cameron, 2006, 2008, Noble et al., 2013b), (ii) capillary action (Anand et al., 2014), (iii) ionic diffusion, (iv) self-potential effect (Smee, 1983; Govett et al., 1984; Goldberg, 1998; Hamilton, 1998; Hamilton et al., 2001, 2004a, 2004b; Timm and Moller, 2001), (v) vaporization, (vi) biology (Dunn, 2007; Anand et al., 2014), (vii) as components of gases, and (viii) transportation by gases (Kristiansson and Malmqvist, 1982; Nilson et al., 1991; Ren et al., 1995; Wang et al., 1995a, 1995b, 1997; Tong et al., 1998; Xie et al., 1999; Noble et al., 2013a, 2013b; Anand et al., 2014). For thin residual cover, any of the mechanisms can contribute to upward metal transport. For exotic cover, or a thick sequence of various overlying post-mineralization rocks and transported regolith, the mechanism of metals migrating upward from buried deposits penetrating through the cover to the surface is still not fully understood. The above-mentioned conceptual models play an important role in understanding the migration mechanism of elements. Although these interpretations focus on the forces driving element migration, they do not discuss the element behavior or metal occurrences during the migration. For instance, an inert element, such as gold, which commonly occurs as dense native grains, would find upward migration difficult.

From the late 1990s to the 2010s, it was realized that nano-scale gold particles may migrate vertically with gas flow and nanoscale metal particles were observed in geogas and soil samples (Wang et al., 1997; Cao et al., 2009; Deditius et al., 2011; Hough et al., 2011; Tong et al., 1998). It still cannot be proved that these nano-scale metal particles come directly from the ore bodies, as bacteria near the surface could also form nano-particles (Banfield and Nealson, 1997; Lower et al., 2001). Recently, nano-scale crystal particles formed in the endogenic processes have been observed (Hough et al., 2008; Noble et al., 2009; Wang and Ye, 2011; Ye et al., 2012). This finding has provided new insight into metal migration mechanism (Wang and Ye, 2011). Nano-geochemistry is one of the most significant research frontiers in geochemical exploration of concealed terrains.

4.2. Nanoparticle migration of native gold and copper through exotic cover

Deep-penetrating geochemical surveys have revealed that anomalies exist at surface over mineral deposits covered by transported regolith. Recently, nanoparticles of metals were widely observed in geogas, soil and ore using a transmission electron microscope (TEM) equipped with an energy dispersive spectroscope (EDS). The observation was implemented at the Laboratory of Microscopy of Peking University. The model of the TEM used in the observation is H9000NAR whose dot resolution is 0.18 nm, lattice resolution is 0.1 nm, minimum spot diameter is 0.8 nm, and accelerating voltage at work is 100–300 kV. And the TEM is equipped with an energy dispersive X-ray spectroscope (EDS), the detecting instrument with ultra-thin window can identify each element whose atomic number falls into the range of 5–92. Components of the particles are determined by the EDS without provision of quality fraction. A spot diameter of <0.2 μm was used in the observation.

Particle diameters ranging from 10 to 200 nm (generally tens of nm) with crystal structure were observed by the TEM. These particles tend to form clusters like a bunch of grapes. In situ analysis by EDS shows that the particles are composed of native copper and alloys of Cu–Fe, Cu–Fe–Mn, Cu–Ag, Cu–Cr, and Cu–Ni and with Si, Al, Ca, O and P from the copper–nickel deposit and Au, Cu–Au, Cu–Fe, and Cu–Ti from the gold deposit. Fig. 13 shows nanoscale hexagonal crystals of Cu and Au alloy from geogases and soil at the Jinwozi goldfield. Fig. 14 shows nanoscale hexagonal crystals of Cu–Ti alloy in (A) geogas, (B) soil and (C) ore at the Zhou'an Cu–Ni deposit. The nanoscale copper and gold particles have hexagonal crystal shape and ordered arrangements of atoms that indicate that they are from the concealed endogenic deposit.

The migration model process illustrated in Fig. 15 can be interpreted that 1) nano-crystal particles of Au and Cu were formed in the mineralized process and released from the ore deposits by weathering during exposure to the surface before covering by transported soils; 2) nano-particles have gas-like characteristic with high diffusivity (Wu, 1998) able enough to overcome gravity force to float in a liquid in underground water saturated zone or in gases in arid terrains; 3) nano-particles have properties with high surface area to volume ratio characterized by a tremendous force able to adsorb onto surface of gas bubbles by surface tension for diffusion with an ascending flow of gas or water bubbles upward to the surface. Such gas bubbles may be derived from

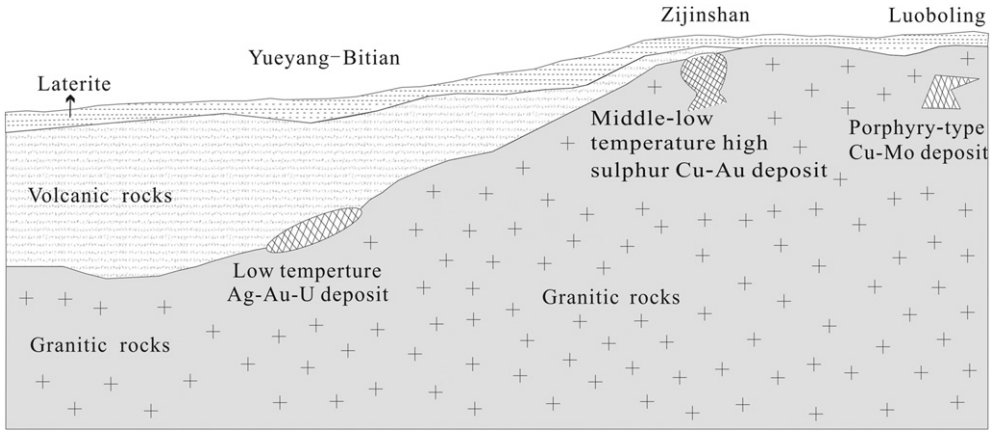

Fig. 9. Typical types of epithermal Ag–Au–U, middle–low temperature hydrothermal Cu–Au, and porphyry Cu–Mo deposit distributed from the southwest to the northeast in the Zijinshan area.

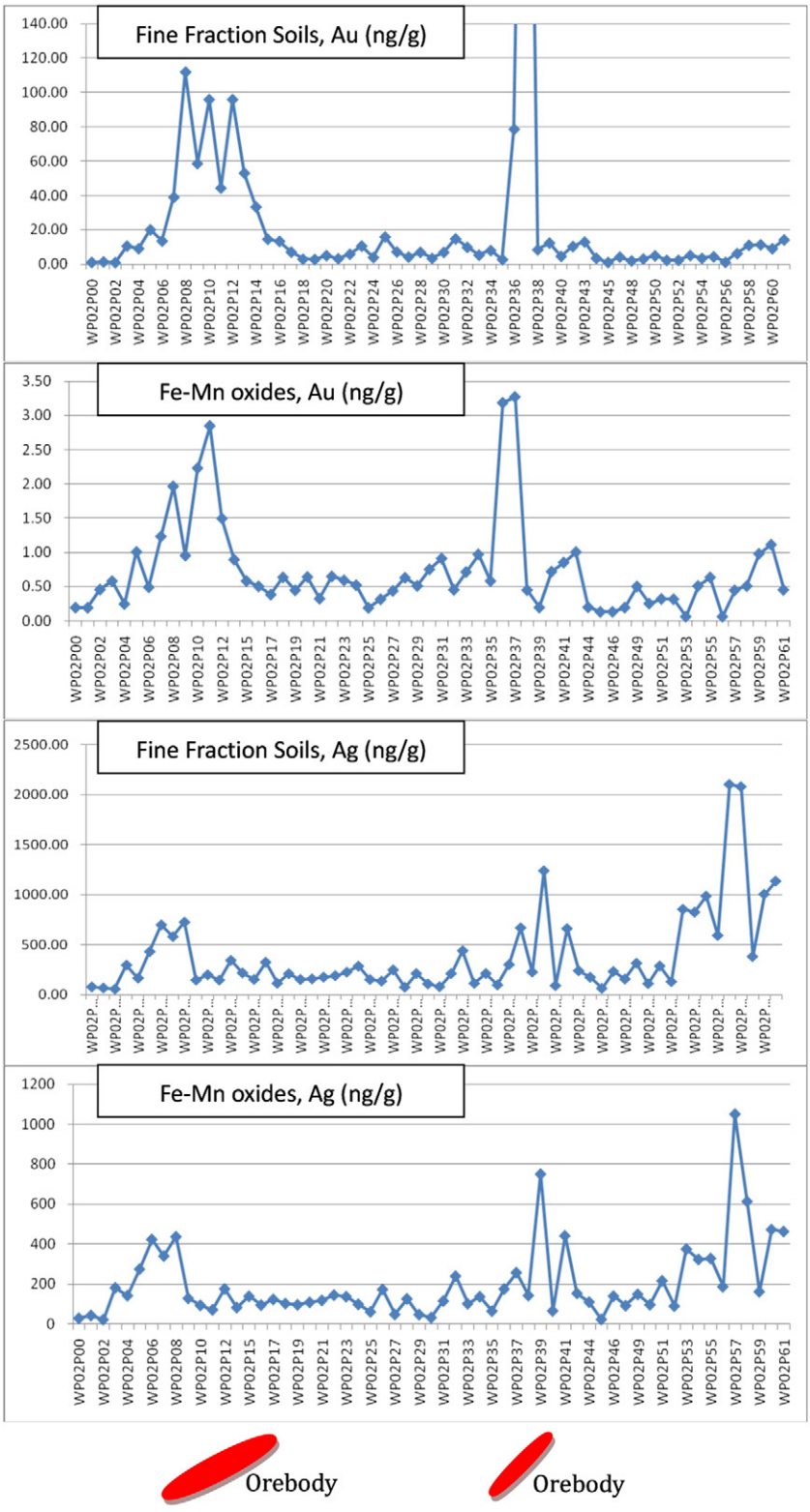

Fig. 10. Anomalies of Au and Ag over the Yueyang Bitian Ag–Au–U deposit at the Zijin Au–Cu field.

the atmosphere and driven to the surface by barometric pumping (Cameron et al., 2004), or be released from the oxidation of sulfide in ore deposits, or from mantle degassing (Gold and Soter, 1980); 4) sedimentary or volcanic rocks and overlying regolith with fractures or pores allow gases and gas-like nanoparticles to migrate upward through covers to the surface; 5) arriving at the surface, some nano-particles may be retained in soil pore gases, and some trapped by soil minerals such as Fe and Mn oxides, clay minerals, colloids, soluble salts and secondary carbonates, and organic matters; and 6) lateral dispersion has been taking place under the surface process of peneplanation. It can be seen from Fig. 6 that high concentrations of gold exist in both coarse- and fine-grained soil fractions at the interface of the bedrock and the overlying soil cover, however, extensive gold anomalies distributed at the surface merely occurred in the fine-grained fraction of soils

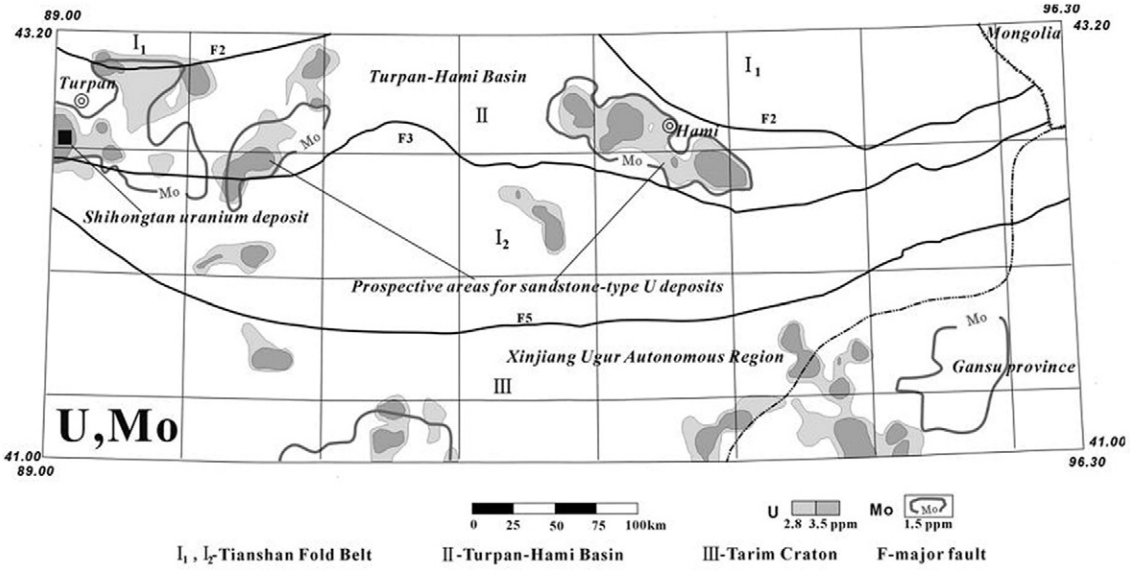

Fig. 11. Geochemical anomalies of U and Mo delineated by wide-spaced sampling of 1 site/100 km^2 at Terpan–Hami Basin, northwestern China (Wang et al., 2007b).

Table 7
Statistics of geochemical data from fine fraction soil samples at Ordos Basin.

Elements	Minimum	Maximum	Average	St. dev.	Background
Ag	40	190	58	11	56
As	3.1	11.8	7.1	1.3	7.1
Cu	9.8	42.9	15.8	3.4	15.2
Hg	4.2	56.7	12.2	5.7	11.0
Mo	0.3	2.1	0.5	0.3	0.4
Pb	14.2	26.7	19.3	2.2	19.2
U	1.4	7.8	2.5	0.7	2.3

Note: Ag, Hg in ng/g, others in μg/g.

(Fig. 6). It can be seen from Fig. 5 that north–south-oriented width of high concentrations of gold at the 210 deposit extends into 5 km, however we know that the altered belt of the 210 ore deposit hosted in the ore-bearing ductile shear zone at Jinwozi gold field is confined in a limited space with a width of tens of meters. It implies that metal particles were led to lateral dispersion after the upward vertical migration from mineralization.

The findings provide nano-scale insight into migration mechanism of deep-penetrating geochemistry and a new method for separation of nanoparticles from soils to search for concealed deposits.

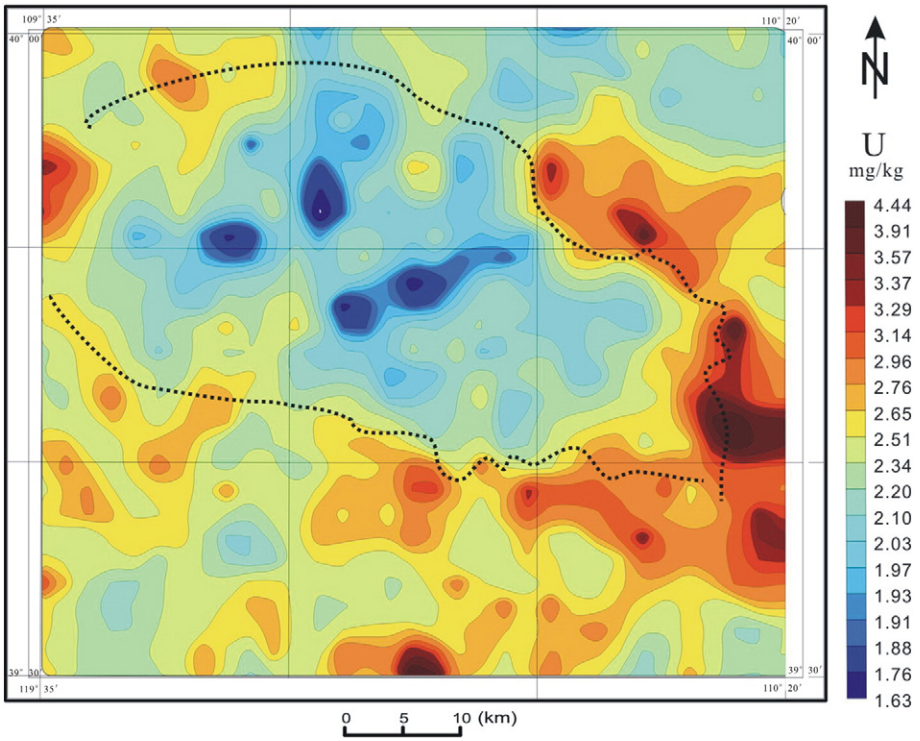

Fig. 12. Geochemical map of U based on the regional geochemical survey in the Ordos Basin, Inner Mongolia, northern China (dashed line indicates U mineralization belt) (Wang et al., 2012).

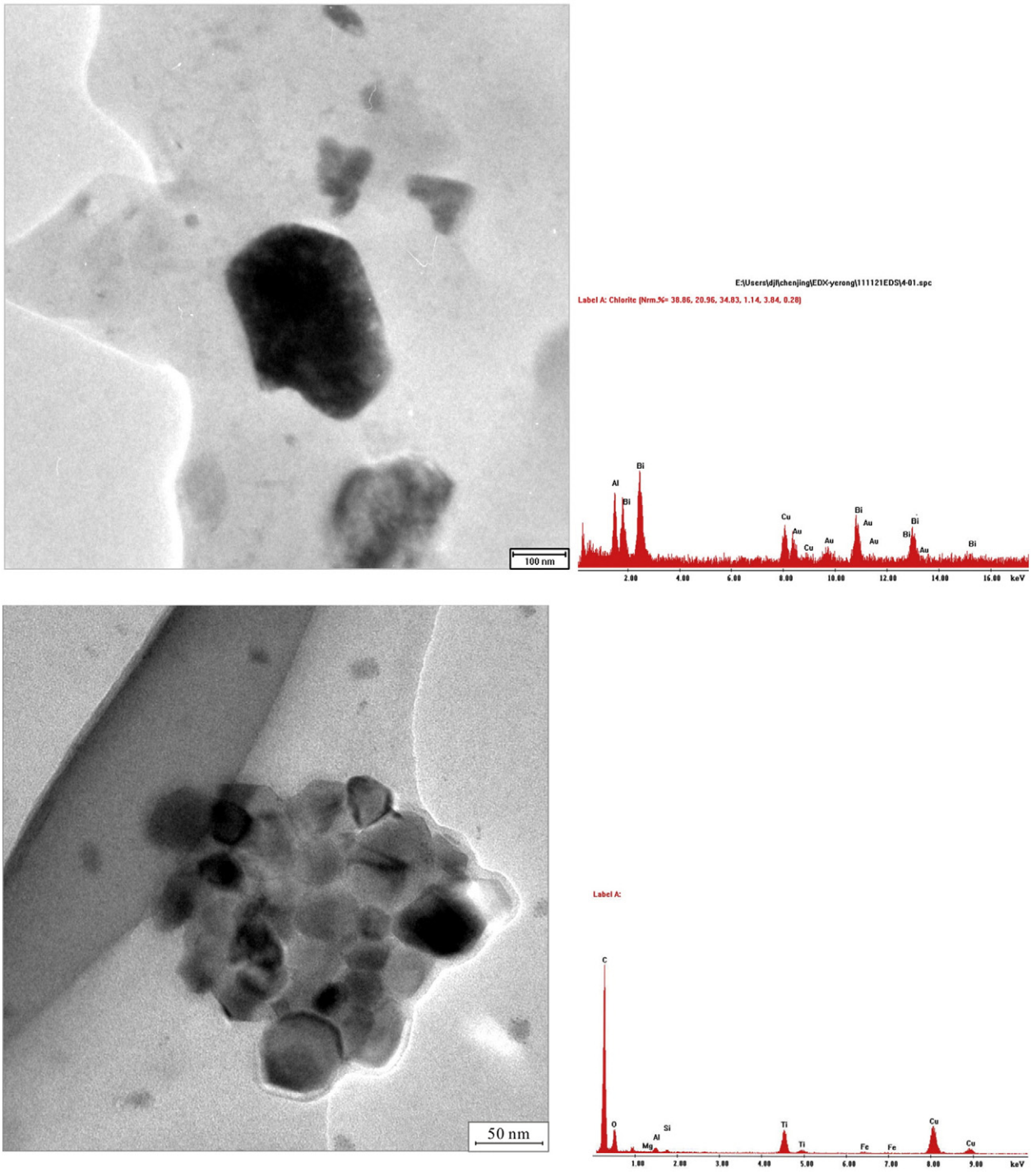

Fig. 13. Nanometer hexagonal crystals of Au–Cu–Bi alloy in geogas and Cu–Ti in soil observed by TEM with EDS over the 210 deposit (Wang and Ye, 2011; Wang et al., 2013).

4.3. Complex uranium migration penetrating sedimentary cover

Why is uranium enriched in the near-surface or surface fine-grained soil? The sequential selective leaching method was used to study the occurrences of uranium in operationally defined forms, i.e., (i) water extractable, (ii) adsorbed and exchangeable onto clay minerals, (iii) occluded in secondary carbonate, and (iv) adsorbed on coatings of Fe–Mn oxides. This showed that uranium is largely adsorbed on clays, which range from 17.9% to 40% (average 30.4%) of the total mineral content of the soil, and occluded in secondary carbonate, which varies from 10.9% to 15.9% (average 13.9%) of the soil (Table 8). Fig. 16 shows that clay minerals tend to increase in the finer soil fractions. The −120 mesh (<0.125 mm) fraction contains the most clay, making up to 40% of the total mineral content. This may indicate that U is converted to uranyl ions [UO_2^{2+}] under oxidizing conditions and is absorbed on clay minerals to accumulate in anomalous concentrations. Uranyl ions [UO_2^{2+}] are easily adsorbed onto clay interlayers. Clay layers have a net negative charge, which is balanced by interlayer cations. Uranyl ions may be converted into anionic hydroxide complexes [$UO_2(OH)_4^{2-}$] at a high pH value. In the presence of carbonate, uranium is further converted to a series of soluble carbonate complexes [$UO_2(CO_3)_3^{4-}$] at an alkaline pH.

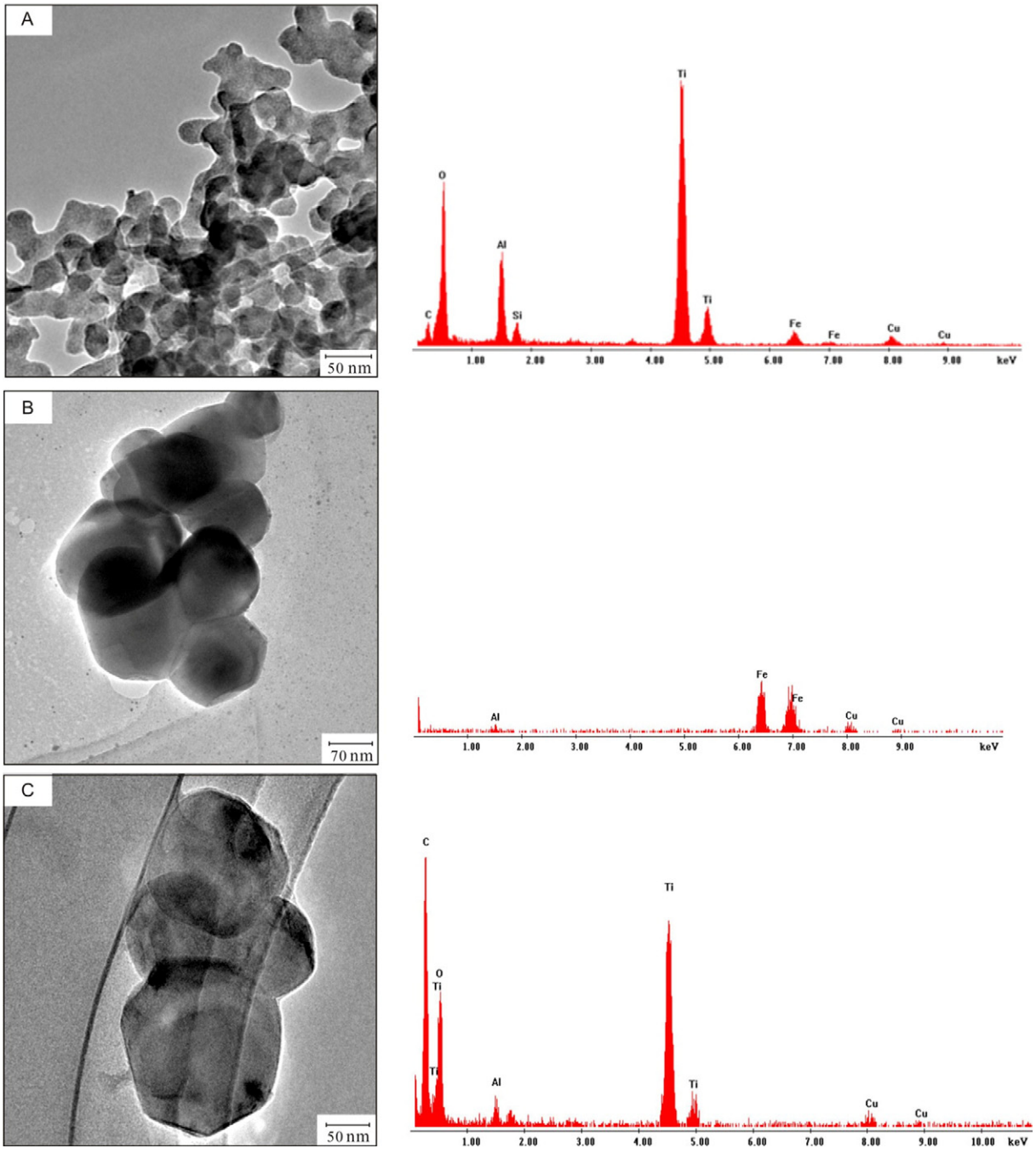

Fig. 14. Nanometer hexagonal crystals of Cu–Ti alloy in (A) geogas, (B) soil and (C) ore observed by TEM with EDS at the Zhou'an Cu–Ni deposit (Wang and Ye, 2011).

5. Discussion and conclusions

The diverse regolith-covered terrains are widely distributed in arid desert peneplains, semi-arid grassland and loess plateaus in northern and northwestern China, forest covered land in the extreme northeast part of China, alluvial plains in eastern China and laterite in southern China. These diverse regolith-covered terrains are unexplored or under-explored, and are the current geochemical challenges for Chinese mineral exploration.

Geochemical exploration research in regolith-covered terrains in China has made great progress both in migration mechanisms and methods during the latest 20 years. Nanoparticles of Cu and Au were widely observed in gases, soils and ores, because these metals occur as native forms whereas U occurs as complex uranyl ions in regolith. This implies that the migration mechanism for different metal elements may be different. Nano-crystals of Cu and Au, formed and liberated from the ore bodies, may migrate with an ascending flow of gases upward to the surface. On arriving at the surface, some of the particles persist in the soil gases and other particles are trapped by soil geochemical barriers such as clays, oxide coatings and colloids. Uranium occurs as complex uranyl ions under oxidizing conditions while migrating from ore bodies to the surface and the ion complexes are absorbed onto clay minerals.

Nanoparticles and ion complexes are more readily absorbed onto fine grains of soils with high contents of clays, colloids, oxides and organic matters. Thus, fine-fraction sampling of regolith combined with selective leaching geochemistry can effectively and efficiently delineate

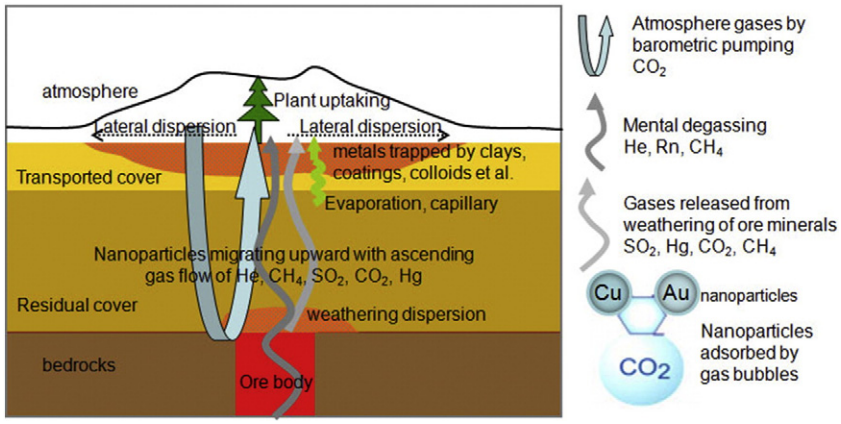

Fig. 15. The comprehensive geochemical model showing vertical migration and lateral dispersion of nano-particles of metals. Modified from Wang et al., 2007b.

Table 8
Concentrations and percentage proportions of uranium in operationally defined sequential selective extraction forms in soil.

Samples	Uranium contents (ppb)					Percentage proportion of (%)			
	WEU	ACU	CU	FMU	T	WEU/T	ACU/T	CU/T	FMU/T
SHT34P0	53.8	954.6	381.3	35.5	2392.5	2.3	39.9	15.9	1.5
SHT34P1	26.7	407.9	228.4	26.4	1712.2	1.6	23.8	13.3	1.5
SHT32P0	57.8	976.9	378.2	47.7	2444.3	2.4	40.0	15.5	1.9
SHT32P1	22.2	331.7	203.4	28.3	1856.8	1.2	17.9	10.9	1.5
Average	40.1	667.8	297.8	34.5	2101.5	1.9	30.4	13.9	1.6

WEU: water extractable; ACM: adsorbed onto clay minerals; CM: soluble carbonate complexes; FMM: adsorbed onto Fe–Mn oxide coatings; T: total U.

geochemical anomalies associated with ore deposits covered by transported cover.

In China, most of the mineral deposits had been discovered by naked eyes before 1980s. Exploration geochemistry has made more important contribution to the new mineral discoveries after 1980s. Fig. 17 shows proportion of 817 new deposits discovered by follow-up exploration for the targets delineated by different methods in China from 1981 to 2000 according to statistic results by the former Ministry of Geology and Mineral Resources of the People's Republic of China. As time goes by, mineral exploration in concealed terrains which occupy 42% of China's territory is becoming important. Fig. 18 shows the number of newly-discovered deposits within the targets delineated by geochemical methods in China from 1981 to 2008 according to statistics by the China Geological Survey. 219 new ore deposits have been discovered at covered terrains from 1981 to 2008, occupying 25% of the total number of 881 new mineral deposits that have been discovered by geochemical methods in China. In addition, for each period of 5 years, this proportion remains at the level of about 20%–40%. The authors concluded that geochemical methods have played and will play more and more important role in mineral discoveries in covered terrains, because geochemistry using laboratory analytical technology can recognize signals from blind mineral deposits, which cannot be seen by human naked eyes. Ore deposits still remain to be discovered by cost-effective surface prospecting methods but the future belongs to those who can effectively and efficiently prospect concealed terrains.

We are still facing some questions: what is the mechanism for other elements? Can the methods be applied to other kinds of mineral deposits? Is it effective for mineral exploration in other regolith-covered terrains such as a loess plateau? Can this method become standardized procedures for mineral exploration? Penetrating geochemistry could step into a brand-new era only by answering the aforementioned and other newly-presented questions.

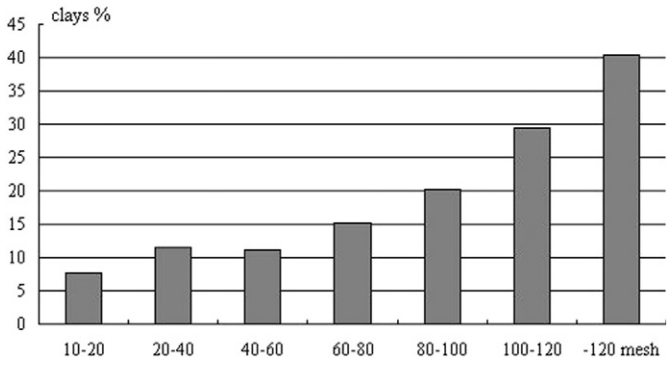

Fig. 16. Percentage proportion of clay minerals in different soil fractions of 10–20, 20–40, 40–86, 60–80, 80–100, 100–120, and −120 mesh (Wang et al., 2011).

Acknowledgments

The authors would like to extend sincere thanks to the Ministry of Land and Resources (Sinoprobe-04-01), the Ministry of Science and Technology (2007AA06Z133), the National Natural Science Foundation of China (No. 1212011120206), and the China Geological Survey (No. 12120115067301 and No. 41203038) for the financial support.

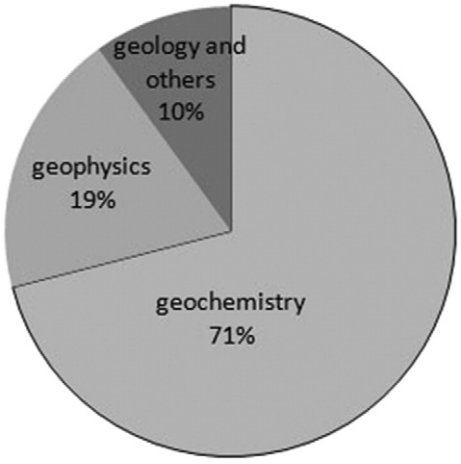

Fig. 17. Pie chart showing proportion of ore deposit targets delineated by different methods.

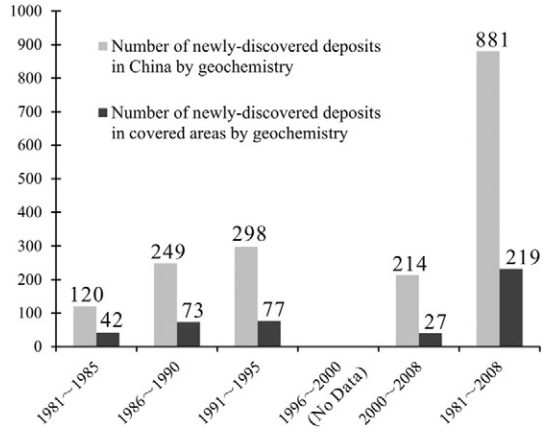

Fig. 18. Bar chart showing the number of newly-discovered deposits within the targets delineated by geochemical methods in China from 1981 to 2008.

References

Anand, R., Cornelius, M., Phang, C., 2007. Use of vegetation and soil in mineral exploration in areas of transported overburden, Yilgarn Craton, western Australia: a contribution towards understanding metal transportation processes. Geochem. Explor. Environ. Anal. 7, 267–288.

Anand, R., Lintern, M., Noble, R., Aspandiar, M., Macfarlane, C., Hough, R., Stewart, A., Wakelin, S., Townley, B., Reid, N., 2014. Geochemical dispersion through transported cover in regolith-dominated terrains — towards an understanding of process. Soc. Econ. Geol. Spec. Publ. 18, 97–126.

Antropova, L.V., Goldberg, I.S., Voroshilov, N.A., Ryss, J.S., 1992. New methods of regional exploration for blind mineralization: application in the USSR. J. Geochem. Explor. 43, 157–166.

Bajc, A.F., 1998. A comparative analysis of enzyme leach and mobile metal ion selective extractions: case studies from glaciated terrain, northern Ontario. J. Geochem. Explor. 61, 113–148.

Banfield, J.F., Nealson, K.H., 1997. Geomicrobiology: Interactions between Microbes and Minerals. Reviews in Mineralogy. Mineralogical Society of America, Washington D.C.

Cameron, E.M., 1998. Deep-Penetrating Geochemistry. Report. Canadian Mining Industry Research Organization (CAMIRO).

Cameron, E.M., Leybourne, M.I., Kelley, D.L., 2002. Exploring for deeply-covered mineral deposits: formation of geochemical anomalies in northern Chile by earthquake-induced surface flooding of mineralized groundwaters. Geology 30, 1007–1010.

Cameron, E.M., Hamilton, S.M., Leybourne, M.I., Hall, G.E.M., McClenaghan, M.B., 2004. Finding deeply buried deposits using geochemistry. Geochem. Explor. Environ. Anal. 4, 7–32.

Cao, J., 2001. The effect factors and the present state of geogas measurement study. Hunan Geol. 20, 154–156 (in Chinese with English abstract).

Cao, J., Hu, R., Liang, Z., Peng, Z., 2009. TEM observation of geogas-carried particles from the Changkeng concealed gold deposit, Guangdong Province, South China. J. Geochem. Explor. 101, 247–253.

Chen, D., Han, X., Na, J., Zhong, T., 1997. Ag-bearing chalcopyrite in the Bitian copper–gold–silver deposit, Fujian. Geol. Rev. 43, 529–534 (in Chinese with English abstract).

Chen, D., Na, J., Xiong, Y., Zhong, T., Li, X., 1998. Sulphosalt minerals and W–Sn sulphides in the Bitian Cu–Au–Ag deposit, Fujian. Acta Geol. Sin. 72, 249–259 (in Chinese with English abstract).

Chen, F., Li, H., Cai, H., Liu, H., 1999. The origin of the Jinwozi gold deposit in eastern Xinjiang — evidence from isotope geochemistry. Geol. Rev. 45, 247–254 (in Chinese with English abstract).

Clark, J.R., 1993. Enzyme-induced leaching of B-horizon soils for mineral exploration in areas of glacial overburden. Trans. Inst. Min. Metall. B Appl. Earth Sci. 102, B19–B29.

Clark, J.R., Meier, A.L., 1990. Enzyme Leaching of Surficial Geochemical Samples for Detecting Hydromorphic Trace Element Anomalies Associated with Precious Metal Mineralized Bedrock Buried Beneath Glacial Overburden in Northern Minnesota.

Clark, J.R., Yeager, J.R., Rogers, P., 1997. Innovative enzyme leach provides cost-effective overburden/bedrock penetration. Proceedings of Exploration 97, pp. 371–374.

Dahlkamp, F.J., 2009. Uranium Deposits of the World (Asia). Springer.

Deditius, A.P., Utsunomiya, S., Reich, M., Kesler, S.E., Ewing, R.C., Hough, R., Walshe, J., 2011. Trace metal nanoparticles in pyrite. Ore Geol. Rev. 42, 32–46.

Dunn, C.E., 2007. Biogeochemistry in mineral exploration. Handbook of Exploration and Environmental Geochemistry 9. Elsevier, Amsterdam (480 pp.).

Erdman, J.A., Olson, J.C., 1985. The use of plants in prospecting for gold: a brief overview with a selected bibliography and topic index. J. Geochem. Explor. 24, 281–304.

Gold, T., Soter, S., 1980. The deep earthgas hypothesis. Sci. Am. 242, 130–138.

Goldberg, I.S., 1998. Vertical migration of elements from mineral deposits. J. Geochem. Explor. 61, 191–202.

Govett, G.J.S., Dunlop, A.C., Atherden, P.R., 1984. Electrogeochemical techniques in deeply weathered terrain in Australia. J. Geochem. Explor. 21, 311–331.

Gray, D.J., Wildman, J.E., Longman, G.D., 1999. Selective and partial extraction analyses of transported overburden for gold exploration in the Yilgarn Craton, Western Australia. J. Geochem. Explor. 67, 51–66.

Hall, G.E.M., 1998. Analytical perspective on trace element species of interest in exploration. J. Geochem. Explor. 61, 1–19.

Hamilton, S.M., 1998. Electrochemical mass transport in overburden: a new model to account for the formation of selective leach geochemical anomalies in glacial terrain. J. Geochem. Explor. 63, 155–172.

Hamilton, S.M., Cameron, E.M., McClenaghan, M.B., Hall, G.E.M., 2001. Deep-Penetrating Geochemistry: Cross Lake Final Report. Report. Canadian Mining Industry Research Organization (CAMIRO) (Report).

Hamilton, S.M., Cameron, E.M., McClenaghan, M.B., Hall, G.E.M., 2004a. Redox, pH and SP variation over mineralization in thick glacial overburden. Part I: methodologies and field investigation at the Marsh Zone gold property. Geochem. Explor. Environ. Anal. 4, 33–44.

Hamilton, S.M., Cameron, E.M., McClenaghan, M.B., Hall, G.E.M., 2004b. Redox, pH and SP variation over mineralization in thick glacial overburden. Part II: field investigation at Cross Lake VMS property. Geochem. Explor. Environ. Anal. 4, 45–58.

Hough, R.M., Noble, R.R.P., Hitchen, G.J., Hart, R., Reddy, S.M., Saunders, M., Clode, P., Vaughan, D., Lowe, J., Gray, D.J., Anand, R.R., Butt, C.R.M., Verrall, M., 2008. Naturally occurring gold nanoparticles and nanoplates. Geology 36, 571–574.

Hough, R.M., Noble, R.R.P., Reich, M., 2011. Natural gold nanoparticles. Ore Geol. Rev. 42, 55–61.

Kristiansson, K., Malmqvist, L., 1982. Evidence for non-diffusive transport of Rn in the ground and a new physical model for the transport. Geophysics 47, 1444–1452.

Kristiansson, K., Malmqvist, L., Persson, W., 1990. Geogas prospecting: a new tool in the search for concealed mineralizations. Endeavour 14, 28–33.

Leybourne, M.I., Cameron, E.M., 2006. Composition of groundwaters associated with porphyry–Cu deposits, Atacama Desert, Chile: elemental and isotopic constraints on water sources and water–rock reactions. Geochim. Cosmochim. Acta 70, 1616–1635.

Leybourne, M.I., Cameron, E.M., 2008. Source, transport, and fate of rhenium, selenium, molybdenum, arsenic, and copper in groundwater associated with porphyry–Cu deposits, Atacama Desert, Chile. Chem. Geol. 247, 208–228.

Lin, X., Wang, X., Zhang, B., Yao, W., 2014a. Multivariate analysis of regolith sediment geochemical data from the Jinwozi gold field, north-western China. J. Geochem. Explor. 137, 48–54.

Lin, X., Zhang, B., Wang, X., 2014b. Application of factor analysis and concentration–volume fractal modeling to delineation of 3D geochemical patterns: a case study of the Jinwozi gold field, NW China. Geochem. Explor. Environ. Anal. 14, 359–367.

Liu, Y., Feng, Q., Yang, R., Fan, A., Xing, X., 2006. Discussion on genesis of sandstone-type uranium deposits in Dongsheng area, Ordos Basin. Acta Geol. Sin. 80, 761–767 (in Chinese with English abstract).

Lower, S., Hochella, M.F., Beverige, T.J., 2001. Bacterial recognition of mineral surfaces: nanoscale interactions between Shewanella and alpha FeOOH. Science 292, 1360–1363.

Luo, X., Li, J., Wu, H., Zhang, P., 1999. A survey of ionic conductivity of soil and its significance in prospecting for ore deposits concealed under thick overburden. J. Geochem. Explor. 66, 307–311.

Luo, X., Hou, B., Wen, M., Zeng, N., Keeling, J., Fidler, R., Fabris, A., 2008. CHIM-geoelectrochemical method in search of concealed mineralization in China and Australia. Chin. J. Geochem. 27, 198–202.

Malmqvist, L., Kristiansson, K., 1985. Physical mechanism for the release of free gases in the lithosphere. Geoexploration 23, 447–453.

Malmqvist, L., Kristiansson, K., Kristiansson, P., 1999. Geogas prospecting—an ideal industrial application of PIXE. Nucl. Inst. Methods Phys. Res. B Beam Interact. Mater. Atoms 150, 484–490.

Mann, A.W., Birrell, R.D., Mann, A.T., 1995. Partial extraction and mobile metal ion. Extended Abstracts of the 17th IGES, pp. 31–34.

Mi, M., Chen, Y., Sun, Y., Wang, Y., Jiang, H., 2009. Rare earth element and platinum-group element geochemistry of the Zhouan Ni–Cu–PGE deposit in Henan province: implications for hydrothermal origin. Acta Petrol. Sin. 25, 2769–2775 (in Chinese with English abstract).

Nilson, R.H., Peterson, E.W., Lie, K.H., 1991. Atmospheric pumping, a mechanism causing vertical transport of contaminated gas through fractured permeable media. J. Geophys. Res. 96, 21933–21948.

Noble, R.R.P., Hough, R.M., Grenik, E.M., 2009. Natural and experimental clues to understand the transport and deposition of supergene gold in western Australia. Explore 142, 1–8.

Noble, R.R.P., Lintern, M.J., Townley, B., Anand, R.R., Gray, D.G., Reid, N., 2013a. Metal migration at the North Miitel Ni sulphide deposit in the southern Yilgarn Craton: part 3, gas and overview. Geochem. Explor. Environ. Anal. 13, 99–113.

Noble, R.R.P., Lintern, M.J., Gray, D.G., Reid, N., Anand, R.R., 2013b. Metal migration at the North Miitel Ni sulphide deposit in the southern Yilgarn Craton: part 1, regolith and groundwater. Geochem. Explor. Environ. Anal. 13, 67–85.

Ozdemir, Z., 2005. *Pinus brutia* as a biogeochemical medium to detect iron and zinc in soil analysis, chromite deposits of the area Mersin, Turkey. Chem. Erde-Geochem. 65, 79–88.

Quan, Z.G., Li, Z.S., 2002. Geological characteristics and genesis of the Shihongtan sandstone-type uranium deposit, Xinjiang. Geol. Rev. 48, 430–436.

Ren, T., Liu, Y., Wang, M., 1995. Nanometer science and hidden mineral resources. Sci. Technol. Rev. 8, 33–36 (in Chinese).

Robertson, I.D.M., 1999. Origins and applications of size fractions of soils overlying the Beasley Creek gold deposit, Western Australia. J. Geochem. Explor. 66, 99–113.

Ryss, J.S., Goldberg, I.S., 1973. The partial extraction of metals (CHIM) method in mineral exploration. Method Tech. 84, 5–19.

Smee, B.W., 1983. Laboratory and field evidence in support of the electrogeochemcially enhanced migration of ions through glaciolacustrine sediment. J. Geochem. Explor. 19, 277–304.

Smith, D.B., Hoover, D.B., Sanzolone, R.F., 1993. Preliminary studies of the CHIM electrogeochemical method at the Kokomo Mine, Russell Gulch, Colorado. J. Geochem. Explor. 46, 257–278.

Timm, F., Moller, P., 2001. The relation between electric and redox potential: evidence from laboratory and field measurements. J. Geochem. Explor. 72, 115–128.

Tong, C., Li, J., 1999. Geogas prospecting and its mechanism in the search for deep-seated or concealed gold deposits. Chin. J. Geophys. 42, 135–142 (in Chinese with English abstract).

Tong, C., Li, J., Liang, X., 1991. Application of INNA to research on the geogas anomaly in a gold deposit, southwest China. Nucl. Sci. Tech. 2, 18–19.

Tong, C., Li, J., Ge, L., Yang, F., 1998. The observation of nanoparticles in geogas and its significance. Sci. China Earth Sci. 28, 153–156.

van Geffen, P.W.G., Kyser, T.K., Oates, C.J., Ihlenfeld, C., 2012. Till and vegetation geochemistry at the Talbot VMS Cu–Zn prospect, Manitoba, Canada: implications for mineral exploration. Geochem. Explor. Environ. Anal. 12, 67–88.

Wang, X., 1998a. Leaching of mobile forms of metals in overburden: development and applications. J. Geochem. Explor. 61, 39–55.

Wang, X., 1998b. Deep penetration exploration geochemistry. Geophys. Geochem. Explor. 22, 166–169 (in Chinese with English abstract).

Wang, X., 1999. Concept, Theoretical Consideration and Methodology of Nanoscale Metals in Earthgas. Geological Publishing House, Beijing, pp. 105–124 (in Chinese).
Wang, X., Ye, R., 2011. Findings of nanoscale metal particles: evidence for deep-penetrating geochemistry. Acta Geosci. Sin. 32, 7–12 (in Chinese with English abstract).
Wang, X., Xie, X., Lu, Y., 1995a. Dynamic collection of geogas and its preliminary application in search for concealed deposits. Geophys. Geochem. Explor. 19, 161–171 (in Chinese with English abstract).
Wang, X., Xie, X., Ye, S., 1995b. Concepts for gold exploration based on the abundance and distribution of ultrafine gold. J. Geochem. Explor. 55, 93–102.
Wang, X., Cheng, Z., Lu, Y., Li, X., Xie, X., 1997. Nanoscale metals in earthgas and mobile forms of metals in overburden in wide-spaced regional exploration for giant ore deposits in overburden terrains. J. Geochem. Explor. 58, 63–72.
Wang, J., Chen, Y., Li, S., Wang, G., Mi, M., 2006a. Geology and genesis of the Zhou'an PGE–Cu–Ni deposit, Henan province. J. Mineral. Petrol. 26, 31–37 (in Chinese with English abstract).
Wang, M., Gao, Y., Zhang, D., Ren, T., Liu, Y., 2006b. Breakthrough in mineral exploration using geogas survey in the basin area of northern Qilian region and its significance. Geophys. Geochem. Explor. 30, 7–12 (in Chinese with English abstract).
Wang, X., Chi, Q., Liu, H., Nie, L., Zhang, B., 2007a. Wide-spaced sampling for delineation of geochemical provinces in desert terrains, northwestern China. Geochem. Explor. Environ. Anal. 7, 153–161.
Wang, X., Wen, X., Ye, R., Liu, Z., Sun, B., Zhao, S., Shi, S., Wei, H., 2007b. Vertical variations and dispersion of elements in arid desert regolith: a case study from the Jinwozi gold deposit, northwestern China. Geochem. Explor. Environ. Anal. 7, 163–171.
Wang, S., Pei, R., Zeng, X., Qiu, X., Wei, M., 2009. Metallogenic series and model of the Zijinshan mining field. Acta Geol. Sin. 83, 145–157 (in Chinese with English abstract).
Wang, X., Xu, S., Zhang, B., Zhao, S., 2011. Deep-penetrating geochemistry for sandstone-type uranium deposits in the Turpan–Hami basin, north-western China. Appl. Geochem. 26, 2238–2246.
Wang, X., Zhang, B., Liu, X., 2012. Nanogeochemistry: deep-penetrating geochemical exploration through cover. Earth Sci. Front. 19, 101–112 (in Chinese with English abstract).
Wang, X., Xu, S., Chi, Q., Liu, X., 2013. Gold geochemical provinces in China: a micro- and nano-scale formation mechanism. Acta Geol. Sin. 87, 1–8 (in Chinese with English abstract).
Wang, X., Zhang, B., Yao, W., Liu, X., 2014. Geochemical exploration: from nanoscale to global-scale patterns. Earth Sci. Front. 21, 65–74 (in Chinese with English abstract).
Williams, T.M., Gunn, A.G., 2002. Application of enzyme leach soil analysis for epithermal gold exploration in the Andes of Ecuador. Appl. Geochem. 17, 367–385.
Wu, B., 1998. Nano-technology and new development of solid physics. Special Issue of Nanometer Sci-Tech and Its Measurement Instruments. Modern Scientific Instruments 55-57(1–2), pp. 34–43 (in Chinese).
Xie, X., Wang, X., 2003. Recent developments on deep-penetrating geochemistry. Earth Sci. Front. 10, 225–238 (in Chinese with English abstract).
Xie, X., Mu, X., Ren, T., 1997. Geochemical mapping in China. J. Geochem. Explor. 60, 99–113.
Xie, X., Wang, X., Li, X., Kremenetsky, A.A., Kheffets, V.K., 1999. Orientation study of strategic deep penetration geochemical methods in the central Kyzylkum desert terrain, Uzbekistan. J. Geochem. Explor. 66, 135–143.
Yan, H., Tang, Z., Qian, Z., Wang, Y., Liu, S., 2011. Zircon U–Pb age and geological significance of Zhou'an copper–nickel sulfide deposit in Henan province. J. Lanzhou Univ. (Nat. Sci.) 47, 23–32 (in Chinese with English abstract).
Yao, W., Wang, X., Zhang, B., Xu, S., Shen, W., Du, X., 2012. Pilot study of deep-penetrating geochemical exploration for sandstone-type uranium deposits, Ordos Basin. Earth Sci. Front. 19, 167–176 (in Chinese with English abstract).
Ye, R., Wang, X., Zhao, L., Chen, D., Fu, Y., 2004. Deep penetration geochemistry methods in Gobi-overburden terrain of the Jinwozi metallogenic belt. Geol. Prospect. 40, 65–70 (in Chinese with English abstract).
Ye, R., Zhang, B., Yao, W., Wang, Y., 2012. Occurrences and formation of copper nanoparticles over the concealed ore deposits. Earth Sci. Front. 19, 120–129 (in Chinese with English abstract).
Yeager, J.R., Clark, J.R., Mitchell, W., Renshaw, R., 1998. Enzyme leach anomalies associated with deep Mississippi Valley-type zinc ore bodies at the Elmwood Mine, Tennessee. J. Geochem. Explor. 61, 103–112.
Yu, X., Shao, Y., Li, Y., 1995. The geological–geochemical prospecting model of the Zijinshan copper–gold deposit and its application. Geophys. Geochem. Explor. 19, 321–331.
Zhang, B., Wang, X., Yao, W., Ye, R., 2013. Technical research of deep-penetrating geochemistry and pilot studies in basins and adjacent areas. Report, pp. 78–118.